

A Facial Reduction Approach for the Single Source Localization Problem

He Shi* Qingna Li†

May 19, 2022

Abstract

The single source localization problem (SSLP) appears in several fields such as signal processing and global positioning systems. The optimization problem of SSLP is nonconvex and difficult to find its globally optimal solution. It can be reformulated as a rank constrained Euclidean distance matrix (EDM) completion problem with a number of equality constraints. In this paper, we propose a facial reduction approach to solve such an EDM completion problem. For the constraints of fixed distances between sensors, we reduce them to a face of the EDM cone and derive the closed formulation of the face. We prove constraint nondegeneracy for each feasible point of the resulting EDM optimization problem without a rank constraint, which guarantees the quadratic convergence of semismooth Newton’s method. To tackle the nonconvex rank constraint, we apply the majorized penalty approach developed by Zhou et al. (IEEE Trans Signal Process 66(3):4331-4346, 2018). Numerical results verify the fast speed of the proposed approach while giving comparable quality of solutions as other methods.

Keywords: Single source localization, Euclidean distance matrix, Facial reduction, Majorized penalty approach, Constraint nondegeneracy

1 Introduction

The single source localization problem (SSLP) has received extensive attentions such as in emergency rescue [30], monitoring [10], tracking and navigating [16], the ad hoc microphone array [25, 17, 14], etc. The objective is to locate a source that is detected by a set of sensors with noisy observations between the source and the sensors. More specifically, given locations $\mathbf{x}_1, \dots, \mathbf{x}_n \in \mathbb{R}^r$ of n sensors (usually $r = 2$ or 3 for visualization) and noisy observation $\delta_{j,n+1} > 0$ between the j -th sensor and unknown source $\mathbf{x}_{n+1} \in \mathbb{R}^r$, where

$$\delta_{j,n+1} = \|\mathbf{x}_j - \mathbf{x}_{n+1}\|_2 + \epsilon_j, \quad j = 1, \dots, n, \quad (1)$$

and ϵ_j is some random noise, we are looking for source $\mathbf{x}_{n+1} \in \mathbb{R}^r$ such that $\|\mathbf{x}_j - \mathbf{x}_{n+1}\|_2$ matches $\delta_{j,n+1}$, $j = 1, \dots, n$ as much as possible.

To seek this approximation, typical vector based models can be summarized into the following least squares model

$$\min_{\mathbf{x}_{n+1} \in \mathbb{R}^r} \sum_{j=1}^n (\|\mathbf{x}_j - \mathbf{x}_{n+1}\|_2^p - \delta_{j,n+1}^p)^2 \quad (2)$$

with $p = 1$ or 2 . Problem (2) is nonconvex, and is in particular nonsmooth in the case of $p = 1$. Different approaches have been developed including the simple fixed point algorithm (SFP), the

*School of Mathematics and Statistics, Beijing Institute of Technology, Beijing, 100081, P. R. China

†Corresponding author. School of Mathematics and Statistics/Beijing Key Laboratory on MCAACI/Key Laboratory of Mathematical Theory and Computation in Information Security, Beijing Institute of Technology, Beijing, 100081, P. R. China. Email: qnl@bit.edu.cn. This author’s research is supported by the National Science Foundation of China (NSFC) 12071032.

sequential weighted least squares algorithm (SWLS) [6], the constrained weighted least squares approach (CWLS) [12] for $p = 1$, and the least square approach based on squared-range measurements (SR-LS) for $p = 2$ [5] in which problem (2) leads to the generalized trust region subproblem (GTRS) that can be solved efficiently and globally.

As a special case of sensor network localization (SNL), SSLP has also been frequently studied in the community of semidefinite programming (SDP) [7, 29, 21, 35, 41]. Let the Gram matrix be defined by $Y := P^\top P$, with $P = [\mathbf{x}_1, \dots, \mathbf{x}_{n+1}] \in \mathbb{R}^{r \times (n+1)}$. By the famous linear transformation $\mathcal{K} : \mathcal{S}^{n+1} \rightarrow \mathcal{S}^{n+1}$ between the positive semidefinite matrices (PSD) cone and the EDM cone [13] defined by

$$\mathcal{K}(Y)_{ij} = Y_{ii} + Y_{jj} - 2Y_{ij},$$

SSLP can be formulated as an SDP with a number of linear constraints

$$\begin{aligned} \min_{Y \in \mathcal{S}^{n+1}} \quad & \frac{1}{2} \|\mathcal{K}(Y) - \Delta\|_F^2 \\ \text{s.t.} \quad & \text{rank}(Y) \leq r \\ & Y e_{n+1} = 0 \\ & Y \in \mathcal{S}_+^{n+1} \\ & \mathcal{K}(Y)_{ij} = \|\mathbf{x}_i - \mathbf{x}_j\|_2^2, \quad 1 \leq i < j \leq n, \end{aligned} \tag{3}$$

where Δ is the given estimated squared distance matrix, $e_{n+1} = (1, \dots, 1)^\top \in \mathbb{R}^{n+1}$, \mathcal{S}^{n+1} denotes the space of $(n+1) \times (n+1)$ real symmetric matrices and \mathcal{S}_+^{n+1} denotes the cone of PSD. Such SDP can be solved by the well-developed SDP packages such as SeDuMi [34], SDPT3 [40] and the recent SDPNAL+ [37] or some specially designed algorithms such as SNLSDP [7] and SFSDP [20].

A separated line of investigating SSLP is from the Euclidean distance matrix (EDM) optimization point of view. The success of EDM models to tackle the distance based optimization problems has been demonstrated in [26, 28, 27] to deal with multidimensional scaling as well as the related problems. Notice that squared distance matrix $D \in \mathcal{S}^{n+1}$ defined by

$$D_{ij} := \|\mathbf{x}_i - \mathbf{x}_j\|_2^2, \quad i, j = 1, \dots, n+1 \tag{4}$$

is an EDM. Here, r is the embedding dimension of D . In [27], Qi et al. proposed a Lagrangian dual method to solve the EDM model (which is equivalent to (2) with $p = 2$):

$$\min_{D \in \mathcal{S}^{n+1}} \quad \frac{1}{2} \|D - \Delta\|_F^2 \tag{5}$$

$$\text{s.t.} \quad -D \in \mathcal{K}_+^{n+1}, \quad \text{diag}(D) = 0 \tag{5a}$$

$$\text{rank}(J_{n+1} D J_{n+1}) \leq r \tag{5b}$$

$$D_{ij} = \|\mathbf{x}_i - \mathbf{x}_j\|_2^2, \quad 1 \leq i < j \leq n, \tag{5c}$$

where $\text{diag}(D)$ is the vector formed by the diagonal elements of D , $\mathcal{K}_+^{n+1} := \{D \in \mathcal{S}^{n+1} \mid v^\top D v \geq 0, \sum_{i=1}^{n+1} v_i = 0\}$, J_{n+1} is the centralization matrix defined as $J_{n+1} := I_{n+1} - \frac{1}{n+1} e_{n+1} e_{n+1}^\top$ with identity matrix $I_{n+1} \in \mathbb{R}^{(n+1) \times (n+1)}$. The basic difference between (3) and (5) is that in (5), one uses (5a) directly to build up the model, rather than using the Gram matrix via \mathcal{K} .

Notice that in SDP model (3) and EDM model (5), there are a lot of equality constraints, describing the fixed distances between sensors. The number of these equality constraints is in the order of $O(n^2)$, which grows fast as n grows. Therefore, how to tackle these equality constraints not only becomes the main concern for SSLP, but also has its own interest in solving models like (3) and (5) more efficiently. Very recently, the facial reduction technique was introduced to tackle the equality constraints in SDP. Specifically, Krislock and Wolkowicz [21] used facial reduction to solve a semi-definite relaxation of SNL, which has been proven to be much faster than the traditional SDP method. In [33], Sremac et al. proposed to reformulate SDP model (3) as the

following SDP problem based on the facial reduction technique

$$\begin{aligned} \min_{Y \in \mathcal{S}^{n+1}} \quad & \frac{1}{2} \|\mathcal{K}(Y) - \Delta\|_F^2 \\ \text{s.t.} \quad & \text{rank}(Y) \leq r \\ & Y \in \text{face}(\Theta, \mathcal{S}_+^{n+1}). \end{aligned} \tag{6}$$

In (6), the known distances between sensors are described in the set of constraints

$$\Theta := \{Y \in \mathcal{S}_+^{n+1} \mid Y e_{n+1} = 0, \mathcal{K}(Y)_{ij} = \Delta_{ij}, 1 \leq i, j \leq n\},$$

and the Gram matrix Y is restricted to the minimal face of PSD (denoted as $\text{face}(\Theta, \mathcal{S}_+^{n+1})$) through facial reduction. Roughly speaking, the minimal face containing a subset is a face that does not contain any other face which contains this subset (See Definition 2.2 for the formal definition). Then (6) reduces to the following SDP model in a smaller scale:

$$\begin{aligned} \min_{R \in \mathcal{S}^{r+1}} \quad & \frac{1}{2} \|\mathcal{K}(CRC^T) - \Delta\|_F^2 \\ \text{s.t.} \quad & \text{rank}(R) \leq r \\ & R \in \mathcal{S}_+^{r+1}, \end{aligned} \tag{7}$$

where $C \in \mathbb{R}^{(n+1) \times (r+1)}$ is a constant matrix. The above two references [27, 33] bring our attentions to the facial reduction technique which we will briefly review.

The idea of facial reduction is to take the intersection of a cone and a set of linear constraints as the constraint on some face of the cone. By characterizing the face property, we can study the corresponding optimization problem restricted on the face of the cone. The faces of cones were investigated since 1980's [4, 8, 9], whereas the research on the face of positive semidefinite (PSD) cone was studied by Hill et al. [19] and the general formulation of PSD faces was derived therein. Very recently, facial reduction techniques have been used in algorithms for several important scenarios including principal component analysis (PCA) [24] and matrix optimization problems [21, 15]. In contrast, the study on faces of the EDM cone is mainly from the theoretical point of view. The EDM cone is the set of EDMs, defined by

$$\mathcal{E}^n = \{D \in \mathcal{S}^n \mid \exists x_1, \dots, x_n \in \mathbb{R}^r, \text{ such that } D_{ij} = \|x_i - x_j\|_2^2, i, j = 1, \dots, n\}.$$

We refer to [32, 42] for other characterizations of the EDM cone. In [38], Tarazaga et al. showed that the faces of the EDM cone are linear mappings of that of the PSD cone, which provides a way to study the faces of the EDM cone. In [39], Tarazaga described the faces of the EDM cone and related these faces to the supporting hyperplane of the EDM cone. In order to further obtain a more explicit expression of the EDM cone, it was proved by Alfakih [1] that faces of the EDM cone is a Gale subspace related to EDM. In his later monograph [2], he derived the minimal face of the EDM cone containing a matrix.

Based on the above analysis, EDM model (5) for SSLP has its advantages over other models like (3). Meanwhile the facial reduction technique reduces a large scale problem (3) to a smaller one in (7), which is also attractive. Therefore, a natural question is whether one can apply the facial reduction technique to EDM model (5). This motivates the work in our paper. Based on EDM model (5) for SSLP, we develop a facial reduction model as follows

$$\begin{aligned} \min_{D \in \mathcal{S}^{n+1}} \quad & \frac{1}{2} \|D - \Delta\|_F^2 \\ \text{s.t.} \quad & \text{rank}(J_{n+1} D J_{n+1}) \leq r \\ & D \in \text{face}(\Omega, \mathcal{E}^{n+1}), \end{aligned} \tag{8}$$

where

$$\Omega := \{D \in \mathcal{E}^{n+1} \mid D_{ij} = \|\mathbf{x}_i - \mathbf{x}_j\|_2^2, 1 \leq i, j \leq n\}, \tag{9}$$

which is equivalent to (5). We show that $\text{face}(\Omega, \mathcal{E}^{n+1})$ can be further characterized by a simple linear constraint $\langle D, H \rangle = 0$, which brings an equivalent facial reduction of (8) and we call it the EDM model based on facial reduction (EDMFR):

$$\min_{D \in \mathcal{S}^{n+1}} \frac{1}{2} \|D - \Delta\|_F^2 \quad (10)$$

$$\text{s.t. } -D \in \mathcal{K}_+^{n+1}, \text{diag}(D) = 0 \quad (10a)$$

$$\text{rank}(J_{n+1} D J_{n+1}) \leq r \quad (10b)$$

$$\langle D, H \rangle = 0. \quad (10c)$$

Compared with (5), the $n(n-1)/2$ linear equality constraints in (5c) is replaced by one linear equality constraint (10c), which significantly reduces the number of equality constraints.

The contributions of our paper are in three folds. Firstly, we derive model (10) for SSLP based on facial reduction. The advantage of EDM model (10) is that it greatly reduces the extra number of equality constraints from $n(n-1)/2$ to one. Secondly, we show constraint nondegeneracy of the convex case of model (10), where the rank constraint is dropped, which makes it possible to solve the corresponding convex problem by the semismooth Newton's method in [26]. Thirdly, inspired by the work in [43], we design a fast algorithm called majorized penalty approach to solve model (10) and verify the competitive performance of the algorithm by various numerical results.

The organization of the paper is as follows. In Section 2, we show how to derive EDMFR (10) from (8). We prove constraint nondegeneracy for the convex relaxation problem of EDMFR in Section 3. In Section 4, we show how to apply the majorized penalty approach to solve (10). In Section 5, we report the numerical results to demonstrate the efficiency of our approach. We conclude the paper in Section 6.

Notations. The interior of \mathcal{S}_+^n is denoted by \mathcal{S}_{++}^n . Let $\text{vec}: \mathcal{S}^n \rightarrow \mathbb{R}_+^{n(n+1)/2}$ map the upper triangular elements of a symmetric matrix to a vector. For $x \in \mathbb{R}^n$, let $\text{Diag}(x)$ be the diagonal matrix consisting of vector x . We denote the null space of a matrix X by $\text{null}(X)$. Finally, we use A_{ij} to denote the (i, j) element in matrix A .

2 Characterization of EDM Face $\text{face}(\Omega, \mathcal{E}^{n+1})$

In this part, we will show how to derive the explicit form of $\text{face}(\Omega, \mathcal{E}^{n+1})$. We need the following definitions including face, exposed face and minimal face, which can be found in Definition 1.1, 1.2 and Theorem 1.27 in [2].

Let C be a convex set in an Euclidean space \mathbb{E} . A convex subset $F \subseteq C$ is a *face* of C , if for any $x, y \in C$ and any point z lying between x and y , one has $z \in F$ implies that $x, y \in F$.

The definitions of exposed face and minimal face are given as follows.

Definition 2.1. *Let C be a convex set in an Euclidean space \mathbb{E} . A face F of C is an exposed face when satisfying one of the following conditions:*

- (i) *There exists a supporting hyperplane \mathcal{H} such that $F = C \cap \mathcal{H}$.*
- (ii) *There exists a vector v satisfying $F = C \cap v^\perp$, where v^\perp is defined by $v^\perp := \{x \in \mathbb{E} \mid \langle v, x \rangle = 0\}$. In this case, we say that v exposes F and v is the exposing vector of F .*

If C is a convex cone, condition (ii) can be reduced to the following condition.

- (iii) *There exists a vector $v \in C^*$ satisfying $F = C \cap v^\perp$, where C^* is the dual cone of C defined by*

$$C^* := \{x^* \in \mathbb{E} \mid \langle x, x^* \rangle \geq 0, \forall x \in C\}.$$

Definition 2.2. [15] *Let C be a convex set in an Euclidean space \mathbb{E} . The minimal face containing a set $S \subseteq C$, denoted as $\text{face}(S, C)$, is the intersection of all faces of C containing S .*

Below we give some simple examples to illustrate the above definitions.

Example 2.3. As shown in Fig. 1, let $C = \{x \in \mathbb{R}^3 \mid 0 \leq x_1, x_2, x_3 \leq 2\}$. $C_1 = \{x \in \mathbb{R}^3 \mid x_3 = 0, 0 \leq x_1, x_2 \leq 2\}$ and $C_2 = \{x \in \mathbb{R}^3 \mid x_2 = 2, 0 \leq x_1, x_3 \leq 2\}$ are faces of C . It can be easily shown that C_1 and C_2 are exposed faces of C . For example, for C_1 , we can find the supporting hyperplane $\mathcal{H} = \{x \in \mathbb{R}^3 \mid x_3 = 0, x_1, x_2 \in \mathbb{R}\}$ such that $C_1 = C \cap \mathcal{H}$. Alternatively, by choosing $v = (0, 0, 1)^\top$, there is $C_1 = C \cap v^\perp$. Therefore, the exposing vector of C_1 is $v = (0, 0, 1)^\top$.

The convex subset $S = \{x \in \mathbb{R}^3 \mid x_2 = 2, (x_1 - 1)^2 + (x_3 - 1)^2 \leq \frac{1}{4}\}$ is not a face of C . However, we can find the minimal face containing S , which is C_2 , i.e., $\text{face}(S, C) = C_2$. It can thus be seen that the minimal face can reduce the feasible region from C to a face of C , which achieve the purpose of dimension reduction.

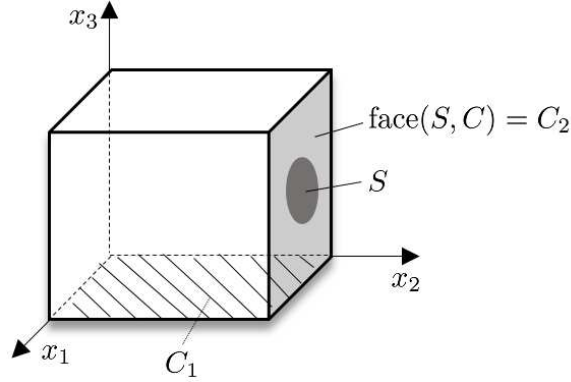


Figure 1: Demonstration of face, minimal face in Example 2.3

It should be pointed out that not all faces are exposed. We give a simple example.

Example 2.4. Consider the convex set $C \subseteq \mathbb{R}^2$ described in Fig. 2, where

$$C = \{x \in \mathbb{R}^2 \mid x_1^2 + x_2^2 \leq 1\} \cup \{x \in \mathbb{R}^2 \mid -1 \leq x_1 \leq 1, -1 \leq x_2 \leq 0\}.$$

Consider the points $y = (-1, 0)^\top$ and $z = (1, 0)^\top$. One can verify that $\{y\}$ and $\{z\}$ are faces of C . $\{y\}$ is not an exposed face of C . The reason is that there is no hyperplane \mathcal{H} , such that $\{y\} = C \cap \mathcal{H}$. Similarly, $\{z\}$ is not an exposed face of C .

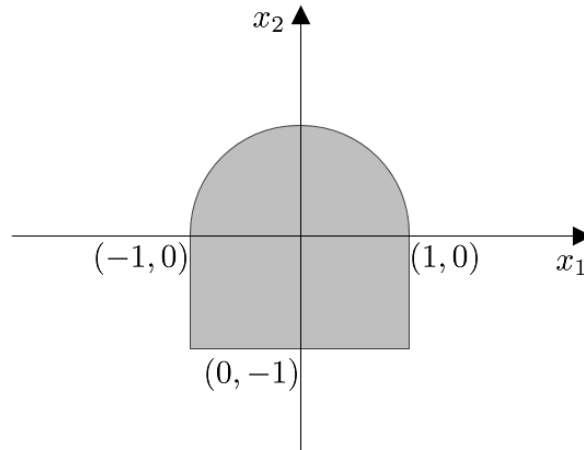


Figure 2: Demonstration of Example 2.4.

Having introduced the definitions related to face above, we are ready to derive the explicit form of $\text{face}(\Omega, \mathcal{E}^{n+1})$. Here Ω is defined as in (9). Since the faces of the EDM cone are exposed

[15, Section 2.1], the minimal face $\text{face}(\Omega, \mathcal{E}^{n+1})$ is exposed as well. As a result, the only thing we need to do is to find the exposing vector of $\text{face}(\Omega, \mathcal{E}^{n+1})$. To that end, we first derive the exposing vector of $\text{face}(\overline{D}, \mathcal{E}^n)$, where $\overline{D} \in \mathcal{S}^n$ is defined by

$$\overline{D}_{ij} = \|\mathbf{x}_i - \mathbf{x}_j\|_2^2, \quad i, j = 1, \dots, n. \quad (11)$$

Then inspired by [33], we extend the result to a higher dimensional case, and derive the exposing vector for $\text{face}(\Omega, \mathcal{E}^{n+1})$. Hence, the derivation of $\text{face}(\Omega, \mathcal{E}^{n+1})$ is divided into the following two steps.

(1) Exposing vector of $\text{face}(\overline{D}, \mathcal{E}^n)$.

To derive the exposing vector of $\text{face}(\overline{D}, \mathcal{E}^n)$, we use the tool of projected Gram matrix. The *projected Gram matrix* Y of \overline{D} is defined by

$$Y := -\frac{1}{2}V^\top \overline{D}V, \quad \text{where } V = \begin{bmatrix} -\frac{1}{\sqrt{n}}e_{n-1}^\top \\ I_{n-1} - \frac{1}{n+\sqrt{n}}e_{n-1}e_{n-1}^\top \end{bmatrix} \in \mathbb{R}^{n \times (n-1)}. \quad (12)$$

It is easy to verify that V satisfies $V^\top e_n = 0$, $V^\top V = I_{n-1}$ and $VV^\top = J_n$.

There are many theories about faces of the EDM cone that have been reflected in [2]. Here we briefly describe the results. The following two definitions are important to characterize the associated hyperplane of $\text{face}(\overline{D}, \mathcal{E}^n)$.

Definition 2.5. (*Gale subspace*) Let $\tilde{D} \in \mathcal{E}^n$ be a given EDM, $P = [p^1 \dots p^n]^\top \in \mathbb{R}^{n \times r}$ be the coordinate matrix, and

$$\begin{bmatrix} P^\top \\ e^\top \end{bmatrix} = \begin{bmatrix} p^1 & \dots & p^n \\ 1 & \dots & 1 \end{bmatrix} \in \mathbb{R}^{(r+1) \times n}.$$

Then the corresponding Gale subspace is

$$G(\tilde{D}) := \text{null} \left(\begin{bmatrix} P^\top \\ e^\top \end{bmatrix} \right) = \text{null}(P^\top) \cap \text{null}(e^\top).$$

Definition 2.6. (*Gale matrix*) If $G(\tilde{D})$ denotes the Gale subspace of an EDM \tilde{D} , then a Gale matrix of \tilde{D} is a matrix whose columns form the basis for $G(\tilde{D})$.

The following lemma relates $\text{face}(\tilde{D}, \mathcal{E}^n)$ to a supporting hyperplane of the EDM cone, which plays an important role in our following analysis.

Lemma 2.7. [2, Theorem 5.8] Let F be a proper face of \mathcal{E}^n . Let $\tilde{D} \in \text{relint}(F)$ and Z_1 be a Gale matrix of \tilde{D} . Let $\mathcal{H} = \{D \in \mathcal{E}^n : \text{trace}(Z_1^\top D Z_1) = 0\}$, then $F = \mathcal{E}^n \cap \mathcal{H}$. Here $\text{relint}(F)$ denotes the relative interior of F .

Lemma 2.8. [31, Theorem 11.6] Let C be a convex set and S be the nonempty convex set of C . In order that there exists a supporting hyperplane \mathcal{H} to C containing S and $C \not\subseteq \mathcal{H}$, if and only if $S \cap \text{relint}(C) = \emptyset$.

Lemma 2.8 leads to the following result.

Lemma 2.9. Let \overline{D} be given by (11) and F be the minimal face of \mathcal{E}^n containing \overline{D} . That is $F = \text{face}(\overline{D}, \mathcal{E}^n)$. Then $\overline{D} \in \text{relint}(F)$.

Proof. For contradiction, if $\overline{D} \notin \text{relint}(F)$, there is $\{\overline{D}\} \cap \text{relint}(F) = \emptyset$. Since $\overline{D} \in F$, \overline{D} is on the relative boundary of F . By Lemma 2.8, there exists a supporting hyperplane (denoted as \mathcal{H}_1) to F and $F \not\subseteq \mathcal{H}_1$. Let $F' = F \cap \mathcal{H}_1$. Consequently,

$$F' \subseteq F, \quad F' \neq F. \quad (13)$$

Now for F' , we have found a supporting hyperplane \mathcal{H}_1 such that $F' = F \cap \mathcal{H}_1$. Therefore, by Definition 2.1 (i), F' is an exposed face of F . Recall that F is a face of \mathcal{E}^n . Together with the fact that faces are transitive [2, Theorem 1.26], we have that F' is also a face of \mathcal{E}^n . Note that $\overline{D} \in F$ and $\overline{D} \in \mathcal{H}_1$, there is $\overline{D} \in F'$. In other words, F' is a face of \mathcal{E}^n containing \overline{D} . By Definition 2.2, F is the intersection of all faces of \mathcal{E}^n containing \overline{D} . Therefore, $F \subseteq F'$. This contradicts with (13). Therefore, $\overline{D} \in \text{relint}(F)$. □

Based on Lemma 2.7, Lemma 2.8 and Lemma 2.9, we can give the explicit form of the exposing vector for $\text{face}(\overline{D}, \mathcal{E}^n)$.

Proposition 2.10. *Let \overline{D} be given by (11) and Y be the projected Gram matrix defined by (12). Define $Z_1 \in \mathbb{R}^{n \times (n-r-1)}$ by*

$$Z_1 := VU, \quad (14)$$

where $U \in \mathbb{R}^{(n-1) \times (n-r-1)}$ is a matrix whose columns form orthonormal bases of $\text{null}(Y)$.¹ Then $-Z_1 Z_1^\top$ exposes $\text{face}(\overline{D}, \mathcal{E}^n)$.

Proof. Let $F := \text{face}(\overline{D}, \mathcal{E}^n)$. By Lemma 2.9, we have $\overline{D} \in \text{relint}(F)$. Therefore, by Lemma 2.7, we can find a hyperplane in which F containing matrix \overline{D} lies. Hence, by the above analysis and Lemma 2.7, we have $\text{face}(\overline{D}, \mathcal{E}^n) = \mathcal{E}^n \cap \mathcal{H}$, where $\mathcal{H} = \{D_1 \in \mathcal{E}^n : \text{trace}(Z_1^\top D_1 Z_1) = 0\}$. In other words,

$$-Z_1 Z_1^\top \in \mathcal{H}^\perp.$$

Next we will prove $-Z_1 Z_1^\top \in (\mathcal{E}^n)^*$. Indeed, we have

$$\begin{aligned} (\mathcal{E}^n)^* &= \{A \in \mathcal{S}^n \mid \langle A, B \rangle \geq 0, \forall B \in \mathcal{E}^n\} \\ &= \{A \in \mathcal{S}^n \mid \langle A, B \rangle \geq 0, \forall B \in \mathcal{K}(\mathcal{S}_+^n)\} \\ &= \{A \in \mathcal{S}^n \mid \langle A, \mathcal{K}(Y) \rangle \geq 0, \forall Y \in \mathcal{S}_+^n\} \\ &= \{A \in \mathcal{S}^n \mid \langle \mathcal{K}^*(A), Y \rangle \geq 0, \forall Y \in \mathcal{S}_+^n\} \\ &= \{A \in \mathcal{S}^n \mid \mathcal{K}^*(A) \in \mathcal{S}_+^n\} \\ &= \{A \in \mathcal{S}^n \mid \text{Diag}(Ae_n) - A \in \mathcal{S}_+^n\}, \end{aligned}$$

where the second equality is due to the fact that $\mathcal{K}(\mathcal{S}_+^n) = \mathcal{E}^n$, as in [15, Page 1163, Line 20] and [33, Page 975, Line 37]. Moreover, there is $\text{Diag}(-Z_1 Z_1^\top e_n) - (-Z_1 Z_1^\top) = Z_1 Z_1^\top$ (Because $Z_1 \in \text{null}(e_n^\top)$). It is obvious that $Z_1 Z_1^\top \in \mathcal{S}_+^n$. Consequently, $-Z_1 Z_1^\top \in (\mathcal{E}^n)^*$.

By the definition of the exposing vector, $-Z_1 Z_1^\top$ exposes $\text{face}(\overline{D}, \mathcal{E}^n)$. The proof is completed. \square

(2) Exposing vector of $\text{face}(\Omega, \mathcal{E}^{n+1})$.

In order to derive the exposing vector of $\text{face}(\Omega, \mathcal{E}^{n+1})$, as in [15, Section 2.3], we consider an undirected graph $G = (V_g, E)$ with vertex set $V_g = \{1, \dots, n, n+1\}$ and edge set $E = \{ij : 1 \leq i < j \leq n\}$. Define projection map $\mathcal{P} : \mathcal{S}^m \rightarrow \mathbb{R}^{n(n+1)/2}$ by

$$\mathcal{P}(A) = (A_{ij})_{ij \in E},$$

i.e., $\mathcal{P}(A)$ is a vector of all entries of A indexed by E . The adjoint of \mathcal{P} is $\mathcal{P}^* : \mathbb{R}^{n(n+1)/2} \rightarrow \mathcal{S}^{n+1}$ defined by

$$(\mathcal{P}^*(y))_{ij} = \begin{cases} y_{ij}/2, & \text{if } i, j \in E \text{ or } j, i \in E, \\ 0, & \text{otherwise.} \end{cases}$$

We have the following result to characterize the exposing vector of $\text{face}(\Omega, \mathcal{E}^{n+1})$.

Theorem 2.11. *Let $v := \text{vec}(-Z_1 Z_1^\top) \in \mathbb{R}^{n(n+1)/2}$, where Z_1 is defined by (14). Let $H = \mathcal{P}^*(v)$, then H exposes $\text{face}(\Omega, \mathcal{E}^{n+1})$.*

Proof. Let $a = \text{vec}(\overline{D}) \in \mathbb{R}_+^{n(n+1)/2}$. By [15, Lemma 4.11], we have

$$-Z_1 Z_1^\top / 2 \text{ exposes } \text{face}(\overline{D}, \mathcal{E}^n) \Leftrightarrow v \text{ exposes } \text{face}(a, \text{vec}(\mathcal{E}^n)).$$

Moreover, we have the following formulation

$$\text{vec}(\mathcal{E}^n) = \mathcal{P}(\mathcal{E}^{n+1}).$$

The feasible domain defined by formula (9) can be rewritten as

$$F = \{D \in \mathcal{E}^{n+1} \mid \mathcal{P}(D) = a\}.$$

¹By [2, Lemma 3.8], Z_1 is a Gale matrix.

Then by [15, Theorem 4.1], we have

$$v \text{ exposes } \text{face}(a, \mathcal{P}(\mathcal{E}^{n+1})) \Leftrightarrow \mathcal{P}^*(v) \text{ exposes } \text{face}(\Omega, \mathcal{E}^{n+1}),$$

where

$$\mathcal{P}^*(v) = \begin{bmatrix} -Z_1 Z_1^\top / 2 & 0 \\ 0 & 0 \end{bmatrix}.$$

In other words, $H = \mathcal{P}^*(v)$ exposes $\text{face}(\Omega, \mathcal{E}^{n+1})$. This completes the proof. \square

Through H , we can perform "null space" representation of $\text{face}(\Omega, \mathcal{E}^{n+1})$. In other words,

$$\text{face}(F, \mathcal{E}^{n+1}) = \mathcal{E}^{n+1} \cap H^\perp. \quad (15)$$

where H^\perp is given by

$$H^\perp := \{D \in \mathcal{S}^{n+1} \mid \langle D, H \rangle = 0\}. \quad (16)$$

With model (8), (15) and (16), we obtain the equivalent problem of model (8)

$$\begin{aligned} \min_{D \in \mathcal{S}^{n+1}} \quad & \frac{1}{2} \|D - \Delta\|_F^2 =: f(D) \\ \text{s.t.} \quad & \text{rank}(J_{n+1} D J_{n+1}) \leq r \\ & D \in \mathcal{E}^{n+1} \cap H^\perp, \end{aligned} \quad (17)$$

which is exactly EDMFR (10). Compare (10) with (5), we recast the $n(n-1)/2$ equality constraints in (5c) by a simple linear constraint $\langle D, H \rangle = 0$, which means that we consider the optimization problem restricted on $\text{face}(\Omega, \mathcal{E}^{n+1})$. Here we summarize the calculation of exposing vector H in Algorithm 1 followed by a toy example.

Algorithm 1 Calculate Exposing Vector H

Input: $\mathbf{x}_1, \dots, \mathbf{x}_n \in \mathbb{R}^r$.

- 1: Calculate $\overline{D} \in \mathcal{S}^n$ by $\overline{D} = \|\mathbf{x}_i - \mathbf{x}_j\|_2^2$, $i, j = 1, \dots, n$.
- 2: Calculate Y by (12).
- 3: Calculate Z_1 by (14).
- 4: Let $H = \begin{bmatrix} -Z_1 Z_1^\top / 2 & 0 \\ 0 & 0 \end{bmatrix}$.

Output: $H \in \mathcal{S}^{n+1}$.

Example 2.12. *The data comes from [5, Example 1]. We consider the case where $n = 5$, i.e., there are five sensor points. We have known sensors points \mathbf{x}_i , distributed in two dimensions, whose coordinate matrix is defined by*

$$\begin{aligned} P & := [\mathbf{x}_1 \ \mathbf{x}_2 \ \mathbf{x}_3 \ \mathbf{x}_4 \ \mathbf{x}_5] \\ & = \begin{bmatrix} 6 & 0 & 5 & 1 & 3 \\ 4 & -10 & -3 & -4 & -3 \end{bmatrix}. \end{aligned}$$

The true coordinate of the source is $\mathbf{x}_6 = (-2, 3)^\top$. To calculate exposing vector H , we need the following steps.

1. Calculate \overline{D} by $\overline{D} = \|\mathbf{x}_i - \mathbf{x}_j\|_2^2$. That is:

$$\overline{D} = \begin{bmatrix} 0 & 232 & 50 & 89 & 58 \\ 232 & 0 & 74 & 37 & 58 \\ 50 & 74 & 0 & 17 & 4 \\ 89 & 37 & 17 & 0 & 5 \\ 58 & 58 & 4 & 5 & 0 \end{bmatrix}.$$

2. Calculate the projected Gram matrix of \bar{D} by

$$Y = -V^\top \bar{D} V / 2 = \begin{bmatrix} 6.8760 & 0.2266 & 1.8570 & 0.6432 \\ 0.2266 & 2.1796 & 0.4886 & 1.1029 \\ 1.8570 & 0.4886 & 2.9208 & 1.3554 \\ 0.6432 & 1.1029 & 1.3554 & 2.0261 \end{bmatrix},$$

where V is calculated by (12).

3. Calculate U by

$$Y =: W \Lambda W^\top.$$

Then $U \in \mathbb{R}^{4 \times 2}$ is the columns in W corresponding to the zero eigenvalues. That is,

$$U = \begin{bmatrix} 0.2145 & 0.0648 \\ 0.7041 & -0.4482 \\ -0.6768 & -0.4313 \\ 0.0126 & 0.7803 \end{bmatrix}.$$

Calculate Z_1 by (14):

$$Z_1 = VU = \begin{bmatrix} -0.1138 & 0.0153 \\ 0.1794 & 0.0696 \\ 0.6689 & -0.4435 \\ -0.7120 & -0.4265 \\ -0.0226 & 0.7851 \end{bmatrix}.$$

4. Exposing vector H is given by

$$H = \begin{bmatrix} -Z_1 Z_1^\top / 2 & 0 \\ 0 & 0 \end{bmatrix} = \begin{bmatrix} -0.0066 & 0.0097 & 0.0415 & -0.0372 & -0.0073 & 0 \\ 0.0097 & -0.0185 & -0.0446 & 0.0787 & -0.0253 & 0 \\ 0.0415 & -0.0446 & -0.3221 & 0.1436 & 0.1816 & 0 \\ -0.0372 & 0.0787 & 0.1436 & -0.3444 & 0.1594 & 0 \\ -0.0073 & -0.0253 & 0.1816 & 0.1594 & -0.3084 & 0 \\ 0 & 0 & 0 & 0 & 0 & 0 \end{bmatrix}.$$

Next, we will show that EDM matrix $D \in \mathcal{S}^6$ between sensors $\mathbf{x}_1, \dots, \mathbf{x}_5$ and source \mathbf{x}_6 is indeed lying on $\text{face}(\Omega, \mathcal{E}^6)$. In fact, D is given by

$$D = \begin{bmatrix} 0 & 232 & 50 & 89 & 58 & 65 \\ 232 & 0 & 74 & 37 & 58 & 173 \\ 50 & 74 & 0 & 17 & 4 & 85 \\ 89 & 37 & 17 & 0 & 5 & 58 \\ 58 & 58 & 4 & 5 & 0 & 61 \\ 65 & 173 & 85 & 58 & 61 & 0 \end{bmatrix} \in \mathcal{S}^6$$

and $\langle D, H \rangle = -1.7764 \times 10^{-14} \approx 0$. Therefore, H is indeed the exposing vector of $\text{face}(\Omega, \mathcal{E}^6)$.

Remark 2.13. To the best of our knowledge, we are the first to use facial reduction technique in EDM model. Based on (10), we solve the EDM model for SSLP on a face of the EDM cone, greatly reducing the number of constraints.

3 Constraint Nondegeneracy for Convex Case

Note that EDMFR (10) is a nonconvex optimization problem due to the rank constraint in (10b). A popular way to deal with the nonconvexity is to simply drop the rank constraint and one will reach a convex EDM model as follows

$$\begin{aligned} \min_{D \in \mathcal{S}^{n+1}} \quad & \frac{1}{2} \|D - \Delta\|_F^2 \\ \text{s.t.} \quad & -D \in \mathcal{K}_+^{n+1} \\ & \mathcal{B}(D) = 0. \end{aligned} \tag{18}$$

Here linear operator $\mathcal{B} : \mathcal{S}^{n+1} \rightarrow \mathbb{R}^{n+2}$ is defined by

$$\mathcal{B}(D) := \begin{bmatrix} \text{diag}(D) \\ \langle D, H \rangle \end{bmatrix}$$

with adjoint operator $\mathcal{B}^* : \mathbb{R}^{n+2} \rightarrow \mathcal{S}^{n+1}$ defined by $\mathcal{B}^*(y) := \text{Diag}(y_{1:n+1}) + y_{n+2}H$.

Problem (18) is essentially in the same form as the EDM model in [26], where $\mathcal{B}(D)$ is replaced by $\text{diag}(D)$. Therefore, to solve (18), one can also apply the semismooth Newton's method, as done in [26]. However, to guarantee the quadratic convergence and the nonsingularity of the generalized Jacobian of the dual problem, one needs constraint nondegeneracy property, which is an essential property behind the good performance of semismooth Newton's method. Therefore, in this section, we will show that constraint nondegeneracy indeed holds for the constraints in (18). Below we first state the definition of constraint nondegeneracy with respect to the constraints in (18). More details about this property for general constraints can be found in [3, 36].

Definition 3.1. [3, Definition 3.2] *Constraint nondegeneracy holds at a feasible point D with respect to the constraints in (18), if the following holds*

$$\mathcal{B} \left(\text{lin}(\mathcal{T}_{\mathcal{K}_+^{n+1}}(D)) \right) = \mathbb{R}^{n+2}, \quad (19)$$

where $\text{lin}(\mathcal{T}_{\mathcal{K}_+^{n+1}}(D))$ denotes the largest linear subspace contained in the tangent cone of \mathcal{K}_+^{n+1} at D .

To show constraint nondegeneracy, we need the following property.

Proposition 3.2. *For $A \in \mathcal{S}^{n+1}$, $\mathbf{a} \in \mathbb{R}^n$, $c \in \mathbb{R}$ and*

$$B := \begin{bmatrix} 0 & \mathbf{a} \\ \mathbf{a}^\top & c \end{bmatrix} \in \mathcal{S}^{n+1},$$

we have

$$\text{trace}(AB) = u_{n+1}^\top A \begin{bmatrix} 2\mathbf{a} \\ c \end{bmatrix},$$

where u_{n+1} represent the $(n+1)$ -th column of $(n+1) \times (n+1)$ identity matrix I_{n+1} .

Proof. With simple calculations, there is

$$\begin{aligned} \text{trace}(AB) &= \sum_{i,j} A_{ij} B_{ij} \\ &= \sum_{i=1}^n A_{i,n+1} B_{i,n+1} + \sum_{j=1}^n A_{n+1,j} B_{n+1,j} + A_{n+1,n+1} c \\ &= \sum_{j=1}^n A_{n+1,j} (2\mathbf{a}_j) + A_{n+1,n+1} c \\ &= u_{n+1}^\top A \begin{bmatrix} 2\mathbf{a} \\ c \end{bmatrix}. \end{aligned}$$

This completes the proof. □

Theorem 3.3. *Constraint nondegeneracy (19) holds for each feasible point D of (18).*

Proof. We divide the proof into two steps.

In step one, we recall the explicit form of $\text{lin}(\mathcal{T}_{\mathcal{K}_+^{n+1}}(D))$ whose result can be obtained from [26]. Let $D \in \mathcal{K}_+^{n+1}$ have the following decomposition:

$$D := Q \begin{bmatrix} \bar{\mathbf{z}}_1 & \bar{\mathbf{z}}_2 \\ \bar{\mathbf{z}}_1^\top & \bar{z}_0 \end{bmatrix} Q, \quad \bar{\mathbf{z}}_1 \in \mathcal{S}^n, \quad \bar{\mathbf{z}}_2 \in \mathbb{R}^n, \quad \bar{z}_0 \in \mathbb{R}, \quad (20)$$

where $Q \in \mathcal{S}^{n+1}$ is the Householder matrix satisfying $Q^2 = I_{n+1}$:

$$Q := I_{n+1} - \frac{1}{n+1 + \sqrt{n+1}} \mathbf{y} \mathbf{y}^\top, \quad \mathbf{y} = (1, \dots, 1, \sqrt{n+1} + 1) \in \mathbb{R}^{n+1}.$$

Let $l := \text{rank}(\bar{Z}_1)$, $\bar{\lambda}_1 \geq \bar{\lambda}_2 \geq \dots \bar{\lambda}_l > 0$ be the positive eigenvalues of \bar{Z}_1 and

$$\bar{Z}_1 = U \begin{bmatrix} \bar{\Lambda} & \\ & 0_{n-l} \end{bmatrix} U^\top, \quad U^\top U = I_l \quad (21)$$

be the spectral decomposition of \bar{Z}_1 , where $\bar{\Lambda} = \text{diag}(\bar{\lambda}_1, \bar{\lambda}_2, \dots, \bar{\lambda}_l) \in \mathcal{S}^l$. Let $\bar{l} := \{1, 2, \dots, l\}$. It can be described by [26, eq. (23)] that the tangent cone of \mathcal{K}_+^{n+1} at D is given as follows

$$\mathcal{T}_{\mathcal{K}_+^{n+1}}(D) := \left\{ Q \begin{bmatrix} U \begin{bmatrix} \Sigma_1 & \Sigma_{12} \\ \Sigma_{12}^\top & \Sigma_2 \end{bmatrix} U^\top & \mathbf{a} \\ \mathbf{a}^\top & a_0 \end{bmatrix} Q : \begin{array}{l} \Sigma_1 \in \mathcal{S}^l, \Sigma_2 \in \mathcal{S}_+^{n-l} \\ \Sigma_{12} \in \mathbb{R}^{l \times (n-l)} \\ \mathbf{a} \in \mathbb{R}^n, a_0 \in \mathbb{R} \end{array} \right\}.$$

Then the largest linear subspace contained in $\mathcal{T}_{\mathcal{K}_+^{n+1}}(D)$ is given by [26, eq. (24)]

$$\text{lin}(\mathcal{T}_{\mathcal{K}_+^{n+1}}(D)) := \left\{ Q \begin{bmatrix} U \begin{bmatrix} \Sigma_1 & \Sigma_{12} \\ \Sigma_{12}^\top & 0 \end{bmatrix} U^\top & \mathbf{a} \\ \mathbf{a}^\top & a_0 \end{bmatrix} Q : \begin{array}{l} \Sigma_1 \in \mathcal{S}^l \\ \Sigma_{12} \in \mathbb{R}^{l \times (n-l)} \\ \mathbf{a} \in \mathbb{R}^n, a_0 \in \mathbb{R} \end{array} \right\}. \quad (22)$$

In step two, we will show (19) holds. By the characterization of $\text{lin}(\mathcal{T}_{\mathcal{K}_+^{n+1}}(D))$ in (22), we can obtain that

$$A = Q \begin{bmatrix} \begin{bmatrix} kI_l & 0 \\ 0 & 0 \end{bmatrix} & \mathbf{a} \\ \mathbf{a}^\top & c \end{bmatrix} Q \in \text{lin}(\mathcal{T}_{\mathcal{K}_+^{n+1}}(D)), \quad \forall [\mathbf{a}^\top, c, k]^\top \in \mathbb{R}^{n+2}.$$

Given arbitrary $\mathbf{b} \in \mathbb{R}^{n+2}$, to show that (19) holds, we want to find $[\mathbf{a}^\top, c, k]^\top \in \mathbb{R}^{n+2}$ such that

$$\mathcal{B}(A) = \mathbf{b}. \quad (23)$$

Let u_i represent the i -th column of $(n+1) \times (n+1)$ identity matrix I_{n+1} . By [26, Theorem 2.3], we have

$$\begin{aligned} A_{ii} &= u_i^\top Q \begin{bmatrix} \begin{bmatrix} kI_l & 0 \\ 0 & 0 \end{bmatrix} & \mathbf{a} \\ \mathbf{a}^\top & c \end{bmatrix} Q u_i \\ &= u_i^\top Q \begin{bmatrix} kI_l & 0 \\ 0 & 0 \end{bmatrix} Q u_i + (u_i)^\top Q \begin{bmatrix} 0 & \mathbf{a} \\ \mathbf{a}^\top & c \end{bmatrix} Q u_i \\ &= \begin{cases} -\frac{1}{\sqrt{n+1}} u_i^\top Q \begin{bmatrix} 2\mathbf{a} \\ c \end{bmatrix} + k, & \text{if } i \leq l, \\ -\frac{1}{\sqrt{n+1}} u_i^\top Q \begin{bmatrix} 2\mathbf{a} \\ c \end{bmatrix}, & \text{otherwise.} \end{cases} \quad (\text{by [26, Theorem 2.3]}) \end{aligned}$$

Hence,

$$\text{diag}(A) = -\frac{1}{\sqrt{n+1}} e_{n+1}^\top Q \begin{bmatrix} 2\mathbf{a} \\ c \end{bmatrix} + \text{diag} \left(\begin{bmatrix} kI_l & 0 \\ 0 & 0 \end{bmatrix} \right).$$

On the other hand, we have

$$\begin{aligned}
\langle A, H \rangle &= \left\langle Q \begin{bmatrix} 0 & \mathbf{a} \\ \mathbf{a}^\top & c \end{bmatrix} Q, H \right\rangle + \left\langle Q \begin{bmatrix} kI_l & 0 \\ 0 & 0 \end{bmatrix} Q, H \right\rangle \\
&= \text{trace} \left(QHQ \begin{bmatrix} 0 & \mathbf{a} \\ \mathbf{a}^\top & c \end{bmatrix} \right) + \text{trace} \left(QHQ \begin{bmatrix} kI_l & 0 \\ 0 & 0 \end{bmatrix} \right) \\
&= u_{n+1}^\top (QHQ) \begin{bmatrix} 2\mathbf{a} \\ c \end{bmatrix} + kl_q \quad (\text{by Proposition 3.2}) \\
&= -\frac{1}{\sqrt{n+1}} e_{n+1}^\top HQ \begin{bmatrix} 2\mathbf{a} \\ c \end{bmatrix} + kl_q \quad (\text{by } Qu_{n+1} = -\frac{1}{\sqrt{n+1}} e_{n+1}) \\
&= kl_q, \quad (\text{by } e_{n+1}^\top H = 0)
\end{aligned}$$

where $l_q := \sum_{i=1}^l (QHQ)_{ii}$. Hence, we have

$$\begin{aligned}
\mathcal{B}(A) &= \begin{bmatrix} \text{diag}(A) \\ \langle A, H \rangle \end{bmatrix} \\
&= \begin{bmatrix} -\frac{1}{\sqrt{n+1}} e_{n+1}^\top Q \begin{bmatrix} 2\mathbf{a} \\ c \end{bmatrix} + kw \\ kl_q \end{bmatrix} \\
&= M \begin{bmatrix} \mathbf{a} \\ c \\ k \end{bmatrix},
\end{aligned}$$

where

$$M := \begin{bmatrix} -\frac{1}{\sqrt{n+1}} Q & w \\ 0 & l_q \end{bmatrix} \begin{bmatrix} 2I_n & 0 \\ 0 & I_2 \end{bmatrix}, \quad w = \text{diag} \left(\begin{bmatrix} I_l & 0 \\ 0 & 0 \end{bmatrix} \right).$$

Since $-H \succeq 0$, then $-QHQ \succeq 0$ with rank $n - r - 1$. Then we have $\sum_{i=1}^l (QHQ)_{ii} \neq 0$. Hence, M is invertible due to the fact that Q is invertible and $l_q \neq 0$.

Hence, for any $\mathbf{b} \in \mathbb{R}^{n+2}$, we can find $[\mathbf{a}^\top, c, k]^\top \in \mathbb{R}^{n+2}$ such that $[\mathbf{a}^\top, c, k]^\top = M^{-1}\mathbf{b}$. For such \mathbf{a} , c and k , we have $\mathbf{b} = \mathcal{B}(A) \in \mathcal{B}(\text{lin}(\mathcal{T}_{\mathcal{K}_+^{n+1}}(D)))$. Thus (19) holds and hence constraint nondegeneracy holds at D . This completes the proof. \square

Constraint nondegeneracy guarantees the quadratic convergence of semismooth Newton's method. We can use the globalized version of semismooth Newton's method proposed in [26] to solve (18). We will take this method into account in Section 5 to conduct our numerical comparison.

4 Majorized Penalty Method for EDMFR

In this section, we will present the numerical algorithm for solving (10), which is the majorized penalty method discussed in [43].

Firstly, we can rewrite (10) as the following compact form

$$\begin{aligned}
\min_{D \in \mathcal{S}^{n+1}} f(D) &:= \frac{1}{2} \|D - \Delta\|_F^2 \\
\text{s.t. } -D &\in \mathcal{K}_+^{n+1}(r) \\
\mathcal{B}(D) &= 0,
\end{aligned} \tag{24}$$

where $\mathcal{K}_+^{n+1}(r)$ is the conditional positive semidefinite cone with rank- r cut defined by

$$\mathcal{K}_+^{n+1}(r) := \{D \in \mathcal{K}_+^{n+1} : \text{rank}(J_{n+1} D J_{n+1}) \leq r\}. \tag{25}$$

Inspired by the majorization technique proposed by [43], we could penalize $\mathcal{K}_+^{n+1}(r)$, and then solve the majorized problem of the resulting problem. Such idea is also used to solve other types of nonconvex models, for example, EDM model with ordinal constraints [23].

4.1 Penalizing $\mathcal{K}_+^{n+1}(\mathbf{r})$

In order to introduce the majorized penalty method in [43], we first give the following lemma which leads to the equivalent reformulation of the rank constraint $D \in \mathcal{K}_+^{n+1}(r)$.

Lemma 4.1. [43, Lemma 2.1] *Given $D \in \mathcal{S}^{n+1}$ and integer $r \leq n+1$. Let $\Pi_{\mathcal{K}_+^{n+1}(r)}^B(D)$ denote the projection of D onto nonconvex set $\mathcal{K}_+^{n+1}(r)$. For any $\Pi_{\mathcal{K}_+^{n+1}(r)}(D) \in \Pi_{\mathcal{K}_+^{n+1}(r)}^B(D)$, we have the following results.*

(i) $\langle \Pi_{\mathcal{K}_+^{n+1}(r)}(D), D - \Pi_{\mathcal{K}_+^{n+1}(r)}(D) \rangle = 0.$

(ii) *The function*

$$h(D) := \frac{1}{2} \|\Pi_{\mathcal{K}_+^{n+1}(r)}(D)\|_F^2$$

is convex and $\Pi_{\mathcal{K}_+^{n+1}(r)}(D) \in \partial h(D)$, where $\partial h(D)$ is the subdifferential of h at D .

(iii) *One particular element of $\Pi_{\mathcal{K}_+^{n+1}(r)}^B(D)$ (denoted by $\Pi_{\mathcal{K}_+^{n+1}(r)}(D)$) is given by*

$$\Pi_{\mathcal{K}_+^{n+1}(r)}(D) = \Pi_{\mathcal{S}_+^{n+1}(r)}(J_{n+1} D J_{n+1}) + (D - J_{n+1} D J_{n+1}).$$

For any $A \in \mathcal{S}_+^{n+1}$, $\Pi_{\mathcal{S}_+^{n+1}(r)}(A)$ can be calculated by

$$\Pi_{\mathcal{S}_+^{n+1}(r)}(A) = \sum_{i=1}^r \max(0, \lambda_i) p_i p_i^\top,$$

with the spectral decomposition of A given by

$$A = \sum_{i=1}^n \lambda_i p_i p_i^\top.$$

The main idea of majorized penalty method [43] is to reformulate constraint $-D \in \mathcal{K}_+^{n+1}(r)$ as the following equivalent form

$$-D \in \mathcal{K}_+^{n+1}(r) \iff g(D) := \frac{1}{2} \text{dist}^2(-D, \mathcal{K}_+^{n+1}(r)) = 0. \quad (26)$$

Here, $\text{dist}(-D, \mathcal{K}_+^{n+1}(r))$ denotes the distance between $-D$ and set $\mathcal{K}_+^{n+1}(r)$. By (26), problem (24) is equivalent to

$$\begin{aligned} \min_{D \in \mathcal{S}^{n+1}} \quad & f(D) \\ \text{s.t.} \quad & g(D) = 0 \\ & \mathcal{B}(D) = 0. \end{aligned} \quad (27)$$

Then we penalize $g(D)$ to the objective function and a majorization method is designed to solve the resulting penalty problem

$$\begin{aligned} \min_{D \in \mathcal{S}^{n+1}} \quad & f_\rho(D) := f(D) + \rho g(D) \\ \text{s.t.} \quad & D \in \Xi, \end{aligned} \quad (28)$$

where $\rho > 0$ is the penalty factor and $\Xi := \{D \in \mathcal{S}^{n+1} \mid \mathcal{B}(D) = 0\}$.

In order to use the majorized penalty method, we have the following result which gives the relationship between $g(\cdot)$ and $h(\cdot)$.

Lemma 4.2. [43, Lemma 2.2] *The function $h(\cdot)$ in Lemma 4.1 can be reformulated by*

$$h(D) = \frac{1}{2} \|D\|_F^2 - g(-D),$$

where $g(D)$ is defined in (26).

Based on the properties above, we need to obtain a majorization function of $g(D)$. Recall the definition of majorization function. A majorization function $g_m(D, A)$ of $g(D)$ at a given point $A \in \mathcal{S}^{n+1}$ satisfies the following conditions

$$g_m(A, A) = g(A), \quad g_m(D, A) \geq g(D), \quad \forall D \in \mathcal{S}^{n+1}.$$

By the convexity of $h(A)$ and $\Pi_{\mathcal{K}_+^{n+1}(r)}(A) \in \partial h(A)$, we have

$$h(D) - h(A) \geq \langle \Pi_{\mathcal{K}_+^{n+1}(r)}(A), D - A \rangle, \quad \forall D \in \mathcal{S}^{n+1}. \quad (29)$$

By (29), the majorization function of $g(D)$ at a given point $A \in \mathcal{S}^{n+1}$ can be obtained by

$$g_m(D, A) := \frac{1}{2} \|D\|_F^2 - h(-A) + \langle \Pi_{\mathcal{K}_+^{n+1}(r)}(-A), D - A \rangle. \quad (30)$$

It can be easily verified that $g_m(D, A)$ is a majorization function of $g(D)$. Then at each iteration D^k , we solve the following subproblem

$$D^{k+1} = \arg \min_{D \in \Xi} f_\rho^m(D) := f(D) + \rho g_m(D, D^k). \quad (31)$$

Majorization function $f_\rho^m(D)$ in (31) can be simplified as

$$\begin{aligned} f_\rho^m(D, D^k) &= \frac{1}{2} \|D\|_F^2 - \langle D, \Delta \rangle + \rho \left(\frac{1}{2} \|D\|_F^2 + \langle \Pi_{\mathcal{K}_+^{n+1}(r)}(-D^k), D \rangle \right) \\ &= \frac{1}{2} \|D\|_F^2 - \langle D, \Delta^k \rangle + \text{const} \\ &= \frac{1}{2} \|D - \Delta^k\|_F^2 + \text{const}, \end{aligned} \quad (32)$$

where $\Delta^k := (\Delta - \rho \Pi_{\mathcal{K}_+^{n+1}(r)}(-D^k)) / (1 + \rho)$ and 'const' represents the constant part with respect to D . Therefore, the subproblem reduces to the following form

$$\min_{D \in \Xi} \frac{1}{2} \|D - \Delta^k\|_F^2. \quad (33)$$

4.2 Solving Subproblem (33) by Explicit Formula.

Subproblem (33) is the projection onto convex set Ξ which admits explicit formula. We derive it below.

The Lagrangian function of problem (33) is given by

$$L(D, y) = \frac{1}{2} \|D - \Delta^k\|_F^2 - \langle \mathcal{B}(D), y \rangle,$$

where $y \in \mathbb{R}^{n+2}$ is the Lagrange multiplier. We can obtain the KKT conditions as follows:

$$\begin{cases} \nabla_D L(D, y) = D - \Delta^k - \mathcal{B}^*(y) = 0 \\ \mathcal{B}(D) = 0. \end{cases}$$

Due to convexity of subproblem (32), we can get the optimal solution by solving the KKT conditions:

$$D^{k+1} := \Delta^k + \mathcal{B}^*(y), \quad (34)$$

where

$$\begin{cases} y_{n+2} = -\frac{\langle \Delta^k - \text{Diag}(\text{diag}(\Delta^k)), H \rangle}{\langle H - \text{Diag}(\text{diag}(H)), H \rangle}, \\ y_{1:n+1} = -\text{diag}(\Delta^k + y_{n+2}^k H). \end{cases} \quad (35)$$

In other words, subproblem (33) admits explicit solution given by (34) and (35). Now we are ready to give the framework of the majorization penalty method for (10).

Note that Algorithm 2 mentioned above is specifically designed for SSLP, which solves EDMFR model (10).

Algorithm 2 FRMPA: Majorized Penalty Approach for EDMFR

Require: Dissimilarity matrix Δ , matrix H , penalty parameter $\rho > 0$, dimension r .

- 1: **Initialize** $D^0 \in \mathcal{E}^{n+1}$ and $k := 0$.
 - 2: **Calculate** D^{k+1} by (34) and (35).
 - 3: **Update** $k \leftarrow k + 1$ and go to Step 2 until convergence.
-

5 Numerical Results

In this section, we will test the semismooth Newton’s method [26] for the convex relaxation model (18) (denoted as convex model with facial reduction technique, **FRC**) and the proposed Algorithm 2 (denoted by **FRMPA**) to see the performance. All the tests are conducted on a laptop in MATLAB R2016a with Intel(R) Core(TM) i5-6200 CPU @ 2.30GHz 2.40GHz, 4GB RAM.

For **FRMPA**, we set the termination condition:

$$f_{prog} := \frac{|f_\rho(D^k) - f_\rho(D^{k-1})|}{1 + f_\rho(D^{k-1})} < 10^{-4}.$$

In other words, when the objective function progresses relatively slowly, we believe that current iteration D^k is a good iteration. In **FRMPA**, we set $\rho = 0.1$. For **FRC**, since the convex problem (18) removes the constraint $\text{rank}(J_{n+1}DJ_{n+1}) \leq r$, the proportion of eigenvalues will be taken into account in the following comparative experiments. We define the proportion as

$$\text{Eigenratio} := \sum_{i=1}^r \lambda_i(-J_{n+1}DJ_{n+1}) / \sum_{i=1}^n \lambda_i(-J_{n+1}DJ_{n+1}),$$

where D is the final computed EDM. The resulting EDM is regarded good if Eigenratio $\geq 90\%$.

After obtaining an EDM D by **FRC** and **FRMPA**, we apply multidimensional scaling (**cMDS**) to obtain a set of data $\hat{\mathbf{x}}_1, \dots, \hat{\mathbf{x}}_n, \hat{\mathbf{x}}_{n+1}$. Together with the coordinates of sensors $\mathbf{x}_1, \dots, \mathbf{x}_n$, we conduct Procrustes process [18] to rotate the sensors back to there original positions, meanwhile, we also obtain the estimated position of the source, denoted by $\bar{\mathbf{x}}_M$.

5.1 Application in Single Source Localization Problem

We compare **FRC** and **FRMPA** with the following methods, the Lagrangian dual method (**LagD**) proposed by [27] for solving problem (5), the facial reduction technique of SDP (**FNEDM**) for solving (3) [33], the squared-range-based least squares (**SR-LS**) [5], the standard fixed point scheme (**SFP**), and the constrained weighted least squares method (**CWLS**) [12]. We report cputime as well as the following measures to evaluate the quality of solutions: squared position error of method M defined by

$$\text{err}_M := \|\mathbf{x}_{n+1} - \bar{\mathbf{x}}_M\|_2^2, \quad (36)$$

where $\bar{\mathbf{x}}_M$ is the estimated location provided by method M .

The following examples are tested for $r = 2$ (E1~E4) and $r = 3$ (E5~E6). Note that **CWLS** is only for $r = 2$.

- E1. [5, Example 1] In this example, we extend Example 2.12 in Section 2 numerically. There is a Gaussian noise ϵ_i with mean 0 and variance of 0.1 between the target node and anchors \mathbf{x}_i , i.e., the noisy distance are $\|\mathbf{x}_{n+1} - \mathbf{x}_i\|_2 + \epsilon_i$. The real and observed distances of target node \mathbf{x}_{n+1} and anchor nodes \mathbf{x}_i are

exact	$\sqrt{65}$	$\sqrt{173}$	$\sqrt{85}$	$\sqrt{58}$	$\sqrt{61}$
noisy	8.0051	13.0112	9.1138	7.7924	8.0210

respectively. The coordinate of the solution by **FRMPA** and **FRC** are both $(-1.9907, 3.0474)$, which is approximately to that of **FNEDM** and **LagD** $(-1.9907, 3.0474)$, while the optimal

solution obtained by SR-LS, SFP and CWLS are $(-2.0189, 2.9585)$, $(-1.9916, 3.0467)$ and $(-1.9895, 3.0431)$, respectively. We demonstrate them in Fig. 3.

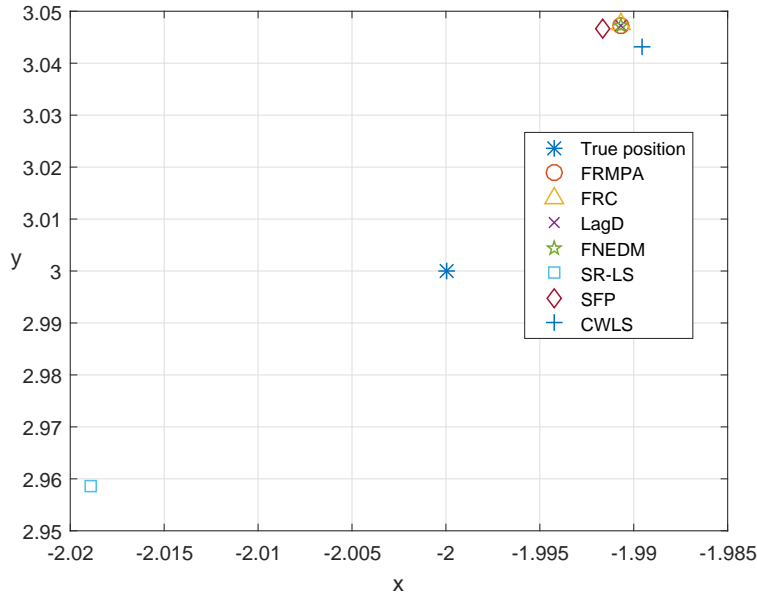


Figure 3: The positions solved by the seven methods in E1

It can be seen from Table 1 that CWLS provides a solution with smallest squared error, while consuming the least cputime. Comparing four solvers FRMPA, FRC, LagD and FNEDM for matrix models of SSLP, they return competitive solutions with almost the same accuracy, whereas our approach FRMPA is the fastest among these four solvers.

Table 1: Numerical results for E1

Method	err	time(s)
FRMPA	2.33E-03	3.32E-03
FRC	2.34E-03	4.05E-03
LagD	2.33E-03	5.56E-02
FNEDM	2.33E-03	4.32E-01
SR-LS	2.08E-03	2.04E-03
SFP	2.32E-03	4.59E-04
CWLS	1.97E-03	4.89E-04

E2. [12] We follow Cheung et al. [12] and consider the sensors as the base stations and the source as the cellular phone. The five base stations are at coordinates $(0, 0)m$, $(3000\sqrt{3}, 3000)m$, $(0, 6000)m$, $(-3000\sqrt{3}, 3000)m$, and $(-3000\sqrt{3}, -3000)m$. In [12], the phone position was fixed at $(1000, 2000)m$.

Consider the distance measurement model in (1). The noises are normally distributed with mean zero and variance σ between 90 and 180. All results are based on an average of 100 instances. As we can see in Fig. 4, the squared position error are very close among the seven methods. In terms of cputime, FRMPA, FRC, SR-LS, SFP and CWLS are all very fast, whereas LagD and FNEDM are not as fast as others.

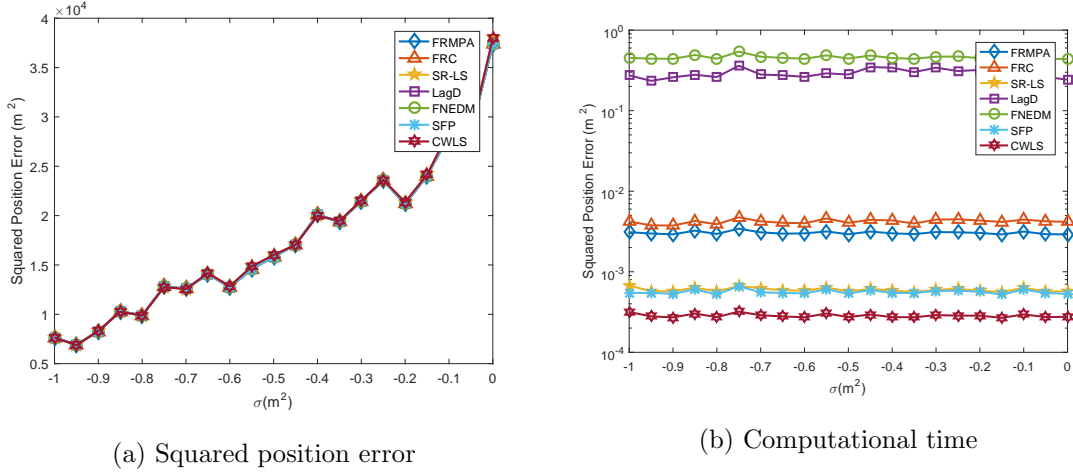


Figure 4: The 2-dimensional results in E2

- E3. [6, Example 4.3] In this example, we randomly generate 100 instances. In each instance, there are five sensors whose positions are \mathbf{x}_i and source position \mathbf{x}_{n+1} are randomly generated from a uniform distribution on $[-10, 10] \times [-10, 10]$. In each instance, there is a normally distributed noise ϵ_i with mean zero and variance σ^2 . In other words, the observed distances between sensors and the source are

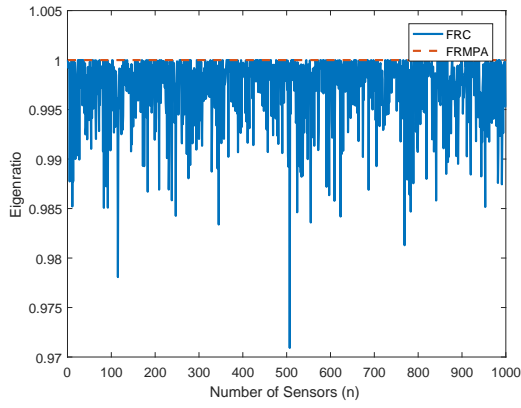
$$\Delta_{n+1,i} = \Delta_{i,n+1} = \|\mathbf{x}_{n+1} - \mathbf{x}_i\|_2 + \epsilon_i, \quad i = 1, \dots, n.$$

The average results over 100 random instances are reported in Table 2. It can be seen from Table 2 that for most cases the optimal solutions obtained by FRC, FRMPA and LagD are very close and they are better than the other four methods. The method FNEDM also performs well in terms of the quality of solutions, however, the cputime is not as fast as FRMPA. For the other three solvers SR-LS, SFP and CWLS, they are very fast yet the quality of the solutions are not as good as FRMPA and LagD.

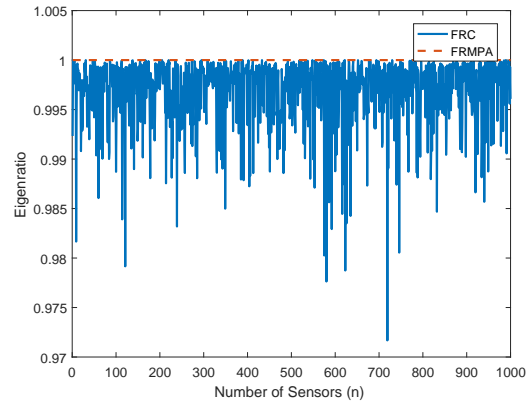
- E4. [6, Example 4.2] In this example, we generate 1000 implementations. In each implementation, sensors \mathbf{x}_j ($j = 1, \dots, n$) and source \mathbf{x}_{n+1} defined by (1) are randomly generated by a uniform distribution on the square $[-1000, 1000] \times [-1000, 1000]$. The observed distances d_j between the sensors and the source are given by (1) where there are normally distributed noises ϵ_j with mean zero and variance 20.

The averaged results are shown in Table 3. We recorded the comparison between FRMPA and the other methods when $n = 4, 5, 8, 10$. The third column is the number of runs out of 1000 in which the solution produced by the method was worse than the FRMPA method in results of err defined in (36). As we can see in Table 3, FRMPA and CWLS have competitive performance, and outperforms other solvers. The reason is explained below. Comparing FRMPA with CWLS, they return similar averaged squared error, whereas FRMPA has more better runs than CWLS over the 1000 random instances. However, CWLS is a bit faster than FRMPA. Compared with FRMPA, FRC does not seem to perform as well as FRMPA because the rank constraint $\text{rank}(-J_{n+1}DJ_{n+1}) \leq r$ is not considered in convex model problem (18). We analyzed the proportions of eigenvalues in the figure and verified our conjecture. As we can see in Fig. 5, Eigenratio of FRMPA is very steady at 100%, while Eigenratio of FRC is not very stable. This explains that why there are some examples that FRC gives larger estimated error than FRMPA does.

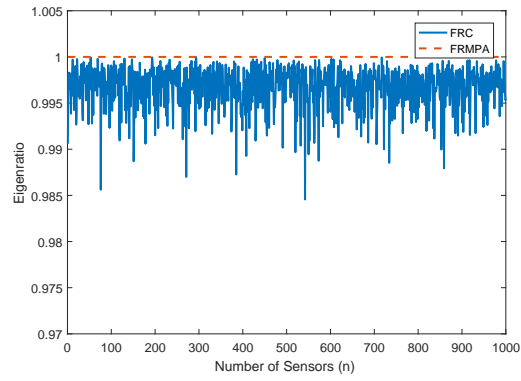
It should be noted that CWLS is only restricted to the case of $r = 2$. Therefore, below, we test some examples with $r = 3$.



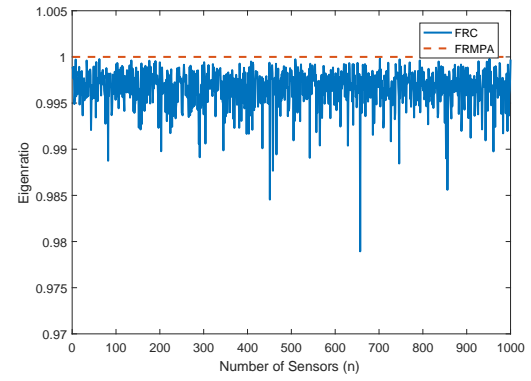
(a) $n = 4$



(b) $n = 5$



(c) $n = 8$



(d) $n = 10$

Figure 5: The comparison results of Eigenratio for FRC and FRMPA in E4

Table 2: Numerical results for E3

Method	σ	1.00E-03	1.00E-02	1.00E-01	1.00E+00
FRMPA	err	1.04E-06	1.05E-04	1.05E-02	1.84E+00
	time(s)	4.30E-03	4.28E-03	5.37E-03	5.19E-03
FRC	err	1.06E-06	1.05E-04	1.05E-02	1.84E+00
	time(s)	4.66E-03	4.57E-03	5.97E-03	7.83E-03
LagD	err	1.07E-06	1.06E-04	1.05E-02	2.88E+00
	time(s)	5.53E-02	5.38E-02	6.60E-02	1.36E-01
FNEDM	err	1.05E-06	1.05E-04	1.05E-02	1.86E+00
	time(s)	7.03E-03	8.33E-03	8.18E-03	8.73E-03
SR-LS	err	1.71E-06	1.70E-04	1.69E-02	2.17E+00
	time(s)	2.13E-03	1.90E-03	2.22E-03	2.20E-03
SFP	err	2.38E+00	2.38E+00	2.41E+00	7.29E+00
	time(s)	9.41E-04	8.34E-04	1.04E-03	1.12E-03
CWLS	err	1.06E-06	1.06E-04	1.05E-02	1.87E+00
	time(s)	4.62E-04	5.52E-04	5.13E-04	4.83E-04

E5. [33] Similar to E2, the sensors \mathbf{x}_j and the source \mathbf{x}_{n+1} are randomly and uniformly distributed in $[-10, 10] \times [-10, 10] \times [-10, 10]$, i.e., $r = 3$. Unlike E2, we randomly generate data with an noise that uniformly distributed, i.e., the observed distances between sensors and the source are

$$\Delta_{n+1,i} = \Delta_{i,n+1} = \|\mathbf{x}_i - \mathbf{x}_{n+1}\|_2(1 + \varepsilon_i),$$

where $\varepsilon_i \in U(-\eta, \eta)$ is a uniformly distributed noise with noise factor η . The relative error c_{re}^M between the true position of the source and the position obtained by method M is given by

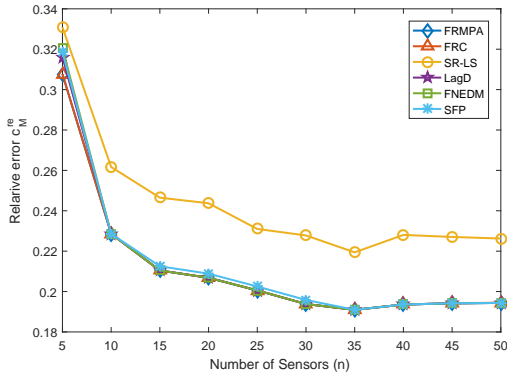
$$c_{re}^M := \frac{\|\bar{\mathbf{x}}_M - \mathbf{x}_{n+1}\|_2}{\|\mathbf{x}_{n+1}\|_2}. \quad (37)$$

We first test the special case of $\eta = 0.2$. Fig. 6 shows that the relative error decreases with the increase of n . The solutions given by SR-LS are not as good as the other methods. For LagD and FNEDM, it takes much more time, however, the other methods remain fast.

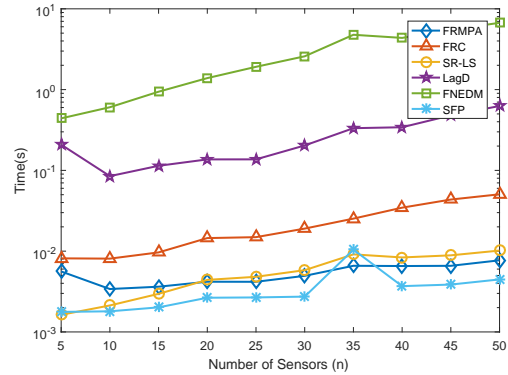
Below we use performance profile to further evaluate the performance of each method. The performance profile is a plot that shows the general performance of all the solvers. The x -axis represents the parameter τ . It represents a ratio between a solver and the winner (such as relative error or cputime). That is, it describes its relative performance. The y -axis represents the probability $\psi_M(\tau)$ of problems for which each solver M can get the best solver through τ . For more details, see [33]. The performance profiles can be seen in Fig. 7. The figure contains the performance profiles for the relative error c_{re}^M and cputime. In most of the cases, Fig. 7a shows that the six methods exhibit approximately good performance. FRMPA obtains the best relative error for almost 100% of the problem instances. LagD and FRC is slightly worse than FRMPA. The chances for the rest of the methods of winning are small, especially for SFP. Therefore, although SFP wins in cputime as demonstrated in Fig. 7b compared with FRMPA, it has a poor performance in relative error. Fig. 7b presents the performance profile for computational time. It seems that SR-LS consumes less time. However, when τ increases, FRMPA requires less time to get the final result. FRC is the fastest of the remaining three matrix optimization methods. FNEDM consumes 10^2 times or even 10^3 times of cputime than that by FRMPA, to achieve similar percentage of success. Compared with the other three EDM formulations FRMPA, FRC and LagD, it is also clear that the SDP formulation consumes more

Table 3: Comparison between FRMPA and the other methods for $n = 4, 5, 8, 10$ in E4

n	Method M	$\text{err}_M > \text{err}_{\text{FRMPA}}$	err_M	time(s)
4	FRMPA	-	2.55E+03	4.29E-03
	FRC	528	2.73E+03	5.68E-03
	LagD	487	3.56E+03	1.13E-01
	FNEDM	510	6.51E+04	4.20E-01
	SR-LS	630	2.92E+03	2.07E+00
	SFP	514	7.97E+04	4.03E-01
	CWLS	500	2.49E+03	4.03E-04
	5	FRMPA	-	6.26E+02
FRC		516	6.26E+02	4.97E-03
LagD		512	6.22E+02	1.16E-01
FNEDM		492	4.68E+04	4.31E-01
SR-LS		663	9.58E+02	3.39E+00
SFP		498	5.87E+04	2.84E-01
CWLS		516	6.35E+02	2.84E-04
8		FRMPA	-	2.69E+02
	FRC	509	2.69E+02	5.46E-03
	LagD	483	2.69E+02	1.60E-01
	FNEDM	506	6.17E+03	5.36E-01
	SR-LS	661	4.39E+02	8.08E-03
	SFP	525	9.88E+03	4.65E-01
	CWLS	507	2.72E+02	4.65E-04
	10	FRMPA	-	2.16E+02
FRC		528	2.16E+02	5.19E-03
LagD		502	2.16E+02	1.60E-01
FNEDM		511	4.88E+03	6.48E-01
SR-LS		652	3.32E+02	1.06E+01
SFP		492	8.22E+03	4.56E-01
CWLS		546	2.18E+02	4.56E-04



(a) Relative error c_{re}^M



(b) Computational time

Figure 6: Numerical results for $\eta = 0.2$ as n changes in E5

time.

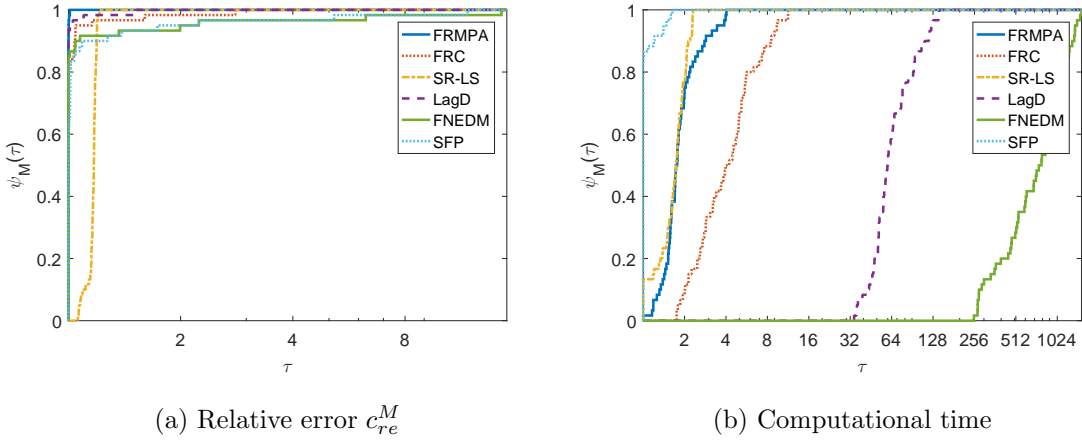
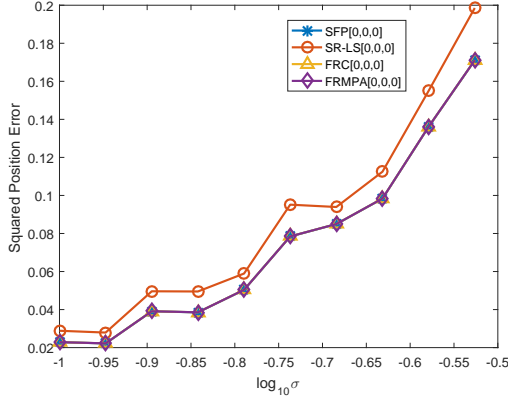
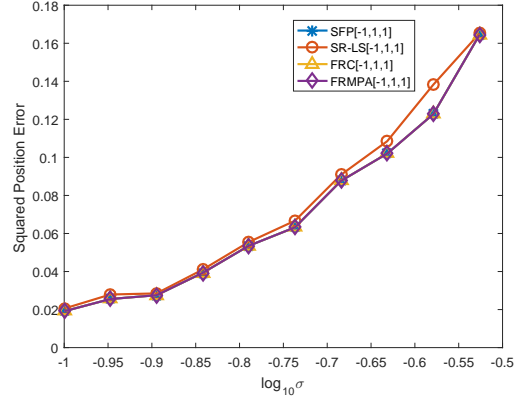


Figure 7: E5: performance profiles for the 100 random tests when $n = [5, 10, 15, 20, 25, 30, 35, 40, 45, 50]$, $\eta = [0.002, 0.005, 0.02, 0.05, 0.2, 0.5]$

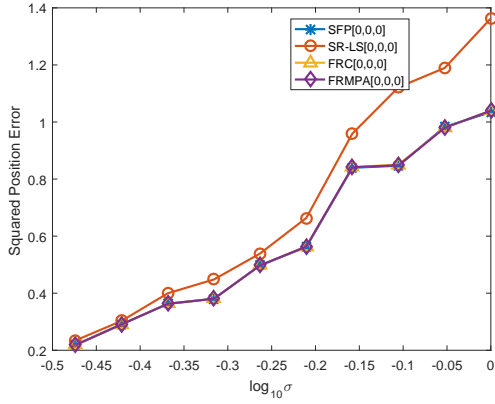
E6. The data are tested in [11, Example 2]. In this example, we consider 3-dimensional case. Consider the distance measurement model in (1). The sensors are $\mathbf{x}_1 = (1, 0, 0)$, $\mathbf{x}_2 = (0, 2, 0)$, $\mathbf{x}_3 = (-2, -1, 0)$, $\mathbf{x}_4 = (0, 0, 2)$, $\mathbf{x}_5 = (0, 0, -1)$. The true source \mathbf{x}_6 is first at $(-1, 1, 1)$ (outside the convex hull of sensors) and then at $(0, 0, 0)$ (inside the convex hull). The noises ϵ_j are normally distributed with mean zero and variance between 10^{-1} and 10^0 . As we found that the 'err' among FRMPA, LagD and FNEDM are almost the same, we only compare FRMPA and FRC with the other two methods (SFP and SR-LS). As we can see in Fig. 8, FRMPA and FRC always have a good estimate whether the source in the convex hull or not. In other words, FRMPA and FRC have more better performance than the other two methods.



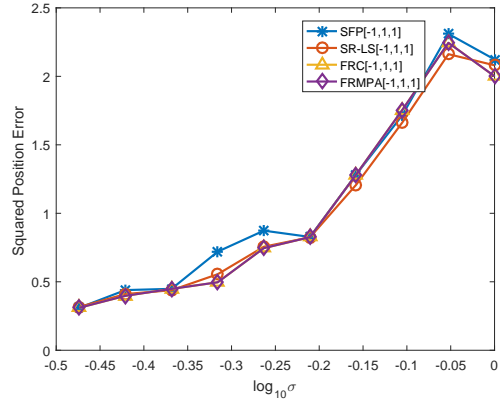
(a) $\sigma \in [10^{-1}, 10^{-0.5}]$



(b) $\sigma \in [10^{-1}, 10^{-0.5}]$



(c) $\sigma \in [10^{-0.5}, 10^0]$



(d) $\sigma \in [10^{-0.5}, 10^0]$

Figure 8: The 3-dimensional error results in E6

To summarize, **FRMPA** and **FRC** are competitive and enjoy advantages in terms of the solution quality and computational time over the rest methods. **FRC** and **FRMPA** sometimes perform similar, for example, E1, E2, E3 and E6. However, in E4 and E5, **FRC** does not seem to perform as well as **FRMPA**. Comparing **FRC** with **FRMPA**, **FRMPA** is faster and more stable since it takes the rank constraint into account.

6 Conclusions

In this paper, we proposed a novel EDM model based on facial reduction. In theory, we derive the minimal face containing constraint (9) and express it as a closed formulation related to its exposing vector. We prove that constraint nondegeneracy is valid for every feasible point in the convex relaxation case. In terms of algorithm, we use the majorized penalty approach proposed by [43] whose subproblem admits closed form solution. The algorithm is simple and efficient. Numerical results show that the EDM model based on facial reduction performs well both in the quality of the solution and the speed.

Acknowledgments. We would like to thank the editor for handling our paper, as well as two anonymous reviewers for their valuable comments, based on which the paper was further improved. We would also like to thank Professor Houduo Qi from the University of Southampton, UK, for his insightful suggestions on the derivation of $\text{face}(\Omega, \mathcal{E}^{n+1})$.

References

- [1] A. Y. Alfakih, A remark on the faces of the cone of Euclidean distance matrices, *Linear Algebra Appl.*, 414(1) (2006) 266-270.
- [2] A. Y. Alfakih, *Euclidean distance matrices and their applications in rigidity theory*, Springer, 2018.
- [3] S. Bai, H. D. Qi, N. Xiu, Constrained best euclidean distance embedding on a sphere: a matrix optimization approach, *SIAM J. Optim.*, 25(1) (2015) 439-467.
- [4] G. P. Barker, Theory of cones, *Linear Algebra Appl.*, 39 (1981) 263-291.
- [5] A. Beck, P. Stoica, J. Li, Exact and approximate solutions of source localization problems, *IEEE Trans. Signal Process.*, 56 (2008) 1770-1778.
- [6] A. Beck, M. Teboulle, Z. Chikishev, Iterative minimization schemes for solving the single source localization problem, *SIAM J. Optim.*, 19 (2008) 1397-1416.
- [7] P. Biswas, T. C. Liang, K. C. Toh, T. C. Wang, Y. Ye, Semidefinite programming approaches for sensor network localization with noisy distance measurements, *IEEE Trans. Autom. Sci. Eng.*, 3 (2006) 360-371.
- [8] J. M. Borwein, H. Wolkowicz, Facial reduction for a cone-convex programming problem, *J. Austral. Math. Soc.*, 30(3) (1981) 369-380.
- [9] J. Borwein, H. Wolkowicz, Regularizing the abstract convex program, *J. Math. Anal. Appl.*, 83(2) (1981) 495-530.
- [10] T. Camp, J. Boleng, V. Davies, A survey of mobility models for ad hoc network research, *Wireless Communications and Mobile Computing*, 2(5) (2010) 483-502.
- [11] M. Chen, D. Zhi, S. Dasgupta, A semidefinite programming approach to source localization in wireless sensor networks, *IEEE Signal Processing Letters*, 15 (2008) 253-256.
- [12] K. W. Cheung, H. C. So, W. K. Ma, Y. T. Chan, A constrained least squares approach to mobile positioning: algorithms and optimality, *EURASIP J. Adv. Signal Process.*, 2006 (2006) 1-23.
- [13] F. Critchley, On certain linear mappings between inner-product and squared-distance matrices, *Linear Algebra Appl.*, 105 (1988) 91-107.
- [14] I. Dokmanic, R. Parhizkar, A. Walther, Y. M. Lu, M. Vetterli, Acoustic echoes reveal room shape, *Proc. Natl. Acad. Sci.*, 110(30) (2013) 12186-12191.
- [15] D. Drusvyatskiy, G. Pataki, H. Wolkowicz, Coordinate shadows of semidefinite and Euclidean distance matrices, *SIAM J. Optim.*, 25(2) (2015) 1160-1178.
- [16] G. Gartner, F. Ortog, *A survey of mobile indoor navigation systems*, Cartography in Central and Eastern Europe, Heidelberg, Germany: Springer, (2010) 305-319.
- [17] N. Gaubitch, W. Kleijn, R. Heusdens, Auto-localization in ad-hoc microphone arrays, *Proc. IEEE Int. Conf. on Acoust. Speech and Signal Processing*, (2013) 106-110.
- [18] G. H. Golub, C. F. Van Loan, *Matrix computations*, Johns Hopkins University Press, Baltimore, 1996.
- [19] R. D. Hill, S. R. Waters, On the cone of positive semidefinite matrices, *Linear Algebra Appl.*, 90 (1987) 81-88.
- [20] S. Kim, M. Kojima, H. Waki, Exploiting sparsity in SDP relaxation for sensor network localization, *SIAM J. Optim.*, 20 (2009) 192-215.

- [21] N. Krislock, H. Wolkowicz, Euclidean distance matrices and applications, In Handbook on semidefinite, conic and polynomial optimization, Springer, Boston, MA, (2012) 879-914.
- [22] J. B. Kruskal, Nonmetric multidimensional scaling: a numerical method, *Psychometrika*, 29(2) (1964) 115-129.
- [23] S. T. Lu, M. Zhang, Q. N. Li, Feasibility and a fast algorithm for euclidean distance matrix optimization with ordinal constraints, *Comput. Optim. Appl.*, 76(2) (2020) 535-569.
- [24] S. Ma, F. Wang, L. Wei, H. Wolkowicz, Robust principal component analysis using facial reduction, *Optim. Eng.*, 21(3) (2020) 1195-1219.
- [25] I. McCowan, M. Lincoln, I. Himawan, Microphone Array Shape Calibration in Diffuse Noise Fields, *IEEE Trans. on Audio, Speech, and Language Processing*, 16(3) (2008) 666-670.
- [26] H. D. Qi, A semismooth Newton method for the nearest Euclidean distance matrix problem, *SIAM J. Matrix Anal. Appl.*, 34(1) (2013) 67-93.
- [27] H. D. Qi, N. Xiu, X. Yuan, A Lagrangian Dual Approach to the Single-Source Localization Problem, *IEEE Tran. Signal Processing*, 61(15) (2013) 3815-3826.
- [28] H. D. Qi, X. Yuan, Computing the nearest Euclidean distance matrix with low embedding dimensions, *Math. Program.*, 147(1-2) (2014) 351-389.
- [29] M. V. Ramana, An exact duality theory for semidefinite programming and its complexity implications, *Math. Program.*, 77(2) (1997) 129-162.
- [30] J. D. Reed, R. M. Buehrer, C. R. C. M. da Silva, An Optimization Approach to Single-Source Localization Using Direction and Range Estimates, *GLOBECOM 2009 - 2009 IEEE Global Telecommunications Conference*, 2009.
- [31] R. T. Rockafellar, *Convex Analysis*, Princeton University Press, Princeton, 1970.
- [32] I. J. Schoenberg, Remarks to Maurice Fréchet's article "Sur la définition axiomatique d'une classed'espaces distanciés vectoriellement applicable sur l'espace de Hilbert", *Ann. Math.*, 36(3) (1935) 724-732.
- [33] S. Sremac, F. Wang, H. Wolkowicz, L. Pettersson, Noisy euclidean distance matrix completion with a single missing node, *J. Glob. Optim.*, 75(4) (2019) 973-1002.
- [34] J. F. Sturm, Using SeDuMi 1.02, a MATLAB toolbox for optimization over symmetric cones, *Optim. Method. Softw.*, 11 (1999) 625-653.
- [35] A. M. C. So, Y. Ye, Theory of semidefinite programming for sensor network localization, *Math. Program.*, 109(2) (2007) 367-384.
- [36] D. Sun, The strong second-order sufficient condition and constraint nondegeneracy in nonlinear semidefinite programming and their implications, *Math. Oper. Res.*, 31(4) (2006) 761-776.
- [37] D. Sun, K. C. Toh, Y. Yuan, X. Y. Zhao, SDPNAL+: A Matlab software for semidefinite programming with bound constraints (version 1.0), *Optim. Method. Softw.*, 35(1) (2020) 87-115.
- [38] P. Tarazaga, T. L. Hayden, J. Wells, Circum-Euclidean distance matrices and faces, *Linear Algebra Appl.*, 232 (1996) 77-96.
- [39] P. Tarazaga, Faces of the cone of Euclidean distance matrices: Characterizations, structure and induced geometry, *Linear Algebra Appl.*, 408 (2005) 1-13.
- [40] Tütüncü, K. C. Toh, M. J. Todd, Solving semidefinite-quadratic-linear programs using sdpt3, *Math. Program.*, 95(2) (2003) 189-217.
- [41] R. M. Vaghefi, J. Schloemann, R. M. Buehrer, NLOS mitigation in TOA-based localization using semidefinite programming, In: *Positioning Navigation and Communication (WPNC)*, (2013) 1-6.
- [42] G. Young, A. S. Householder, Discussion of a set of points in terms of their mutual distances, *Psychometrika*, 3(1) (1938) 19-22
- [43] S. Zhou, N. Xiu, H. D. Qi, A fast matrix majorization-projection method for penalized stress minimization with box constraints, *IEEE Trans. Signal Process.*, 66(16) (2018) 4331-4346.